



Diurnal Patterns in the Observed Cloud Liquid Water Path Response to Droplet Number Perturbations

Kevin M. Smalley^{1†}, Matthew D. Lebsock¹, and Ryan Eastman²

¹Jet Propulsion Laboratory, California Institute of Technology.

²Department of Atmospheric Sciences, University of Washington, Seattle, Washington, USA

Contents of this file

Tables S1 to S2
Figures S1 to S4

Additional Supporting Information (Files uploaded separately)

Captions for Table S2 Caption: The λ values calculated in prior observational and LES studies shown in Figure 4. They are colored by if they represent non-precipitating, **precipitating**, or **indiscriminate** situations (*Table_S2_lwp_adj_GRL_manuscript.xlsx*).

Introduction

Figure S1 shows how cloud-droplet number concentration retrieved using the Advanced-Baseline Imager (ABI) onboard GOES-16 compares to MODIS and CALIPSO. Each data product is discussed in detail and this figure is explained in Section 2.3 of the main text.

Figure S2 shows the lookup table we used to statistically determine the probability of precipitation and precipitation rate along all trajectories. This was done by colocating AMSR-2 warm precipitation rates (described in section 2.5 of the main text) with ABI, and then binning precipitation occurrence and precipitation rate (including non-raining pixels i.e. 0 mm Day⁻¹) by corrected ABI LWP and uncorrected ABI N_d. We then map each LWP and N_d value back to this lookup table to determine statistically the precipitation probability and rate. In general, we find that the likelihood of precipitation and

precipitation rates increase mostly as a function of increasing LWP, with rain likelihood approaching 100% at $LWP > 100 \text{ g m}^{-2}$ and maximum rain rates occurring at $LWP > 200 \text{ g m}^{-2}$.

Figure S3 demonstrates how we calculate $\frac{d\ln(CLWP)}{d\ln(N_d)} (\lambda)$. Specifically, we bin all trajectories by their starting LWP, and fit a line to all $(\ln(LWP[\text{at each time}]) - \ln(LWP[\text{time} = 0]))$ and $\ln(N_d[\text{time} = 0])$ values within that bin. We then consider the slope of each fitted line, at each time as λ . This is described in detail in Section 2.6 in the main text.

Figure S4 shows each individual curve shown in Figure 1 of the main text. Note, the **red points** represent linearly interpolated λ values at night. This was necessary, because, although we are analyzing three years of data, there is not enough microwave LWP data to fill in all times at night. Therefore, to calculate the autocorrelation function for each sensitivity curve shown in Figure 2, we needed to fill in the gaps at night along each curve.

Table S1 shows the microwave imagers that are colocated with all trajectories analyzed to determine how cloud liquid water path (LWP) changes at night. This data and how we process it are described in Section 2.2 of the main text.

Table S2 shows how λ vary among prior literature. Each study is initially separated by whether they are conducted using observations or large-eddy simulations (LES), what each λ value (second column) represents is detailed in column 3, and if each λ value is representative of precipitating or non-precipitating conditions are colored in red and black respectively. Note, any λ colored blue represents situations where we could not confidently determine if it represents non-precipitating or precipitating conditions. In the main text, the observed values are binned in the Obs. column of Figure, and the LES values are binned in the LES column of Figure 4.

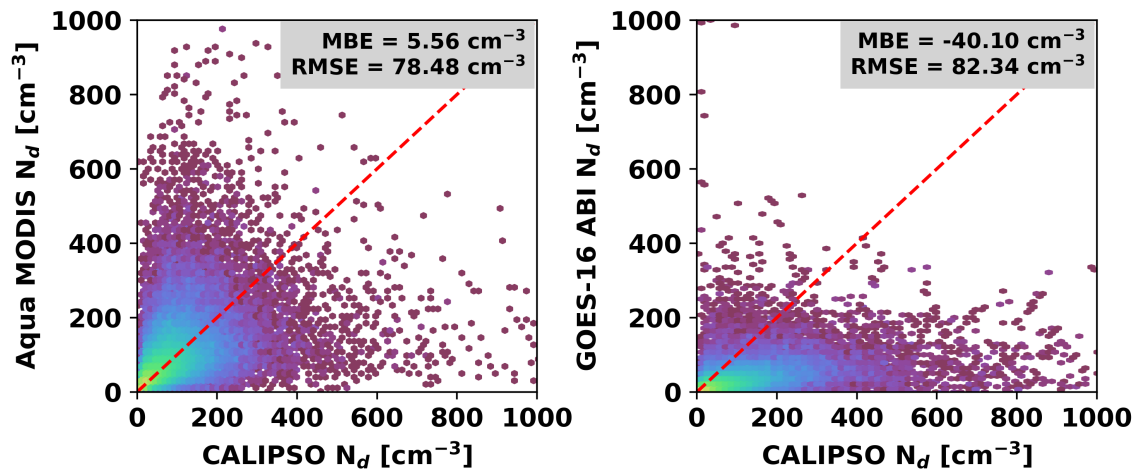


Figure S1. Collocated Aqua MODIS and Calipso cloud-top N_d are shown in (a), and collocated GOES-16 ABI and CALIPSO N_d are shown in (b).

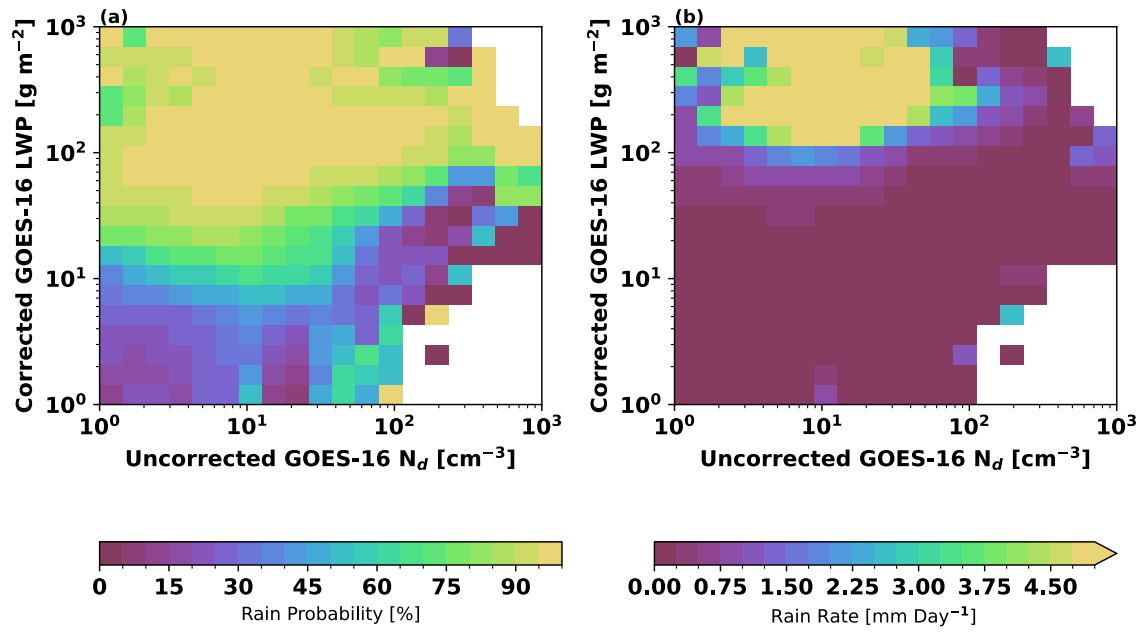


Figure S2. Colocated GOES-16 and AMSR-2 mean precipitation rate and probability of precipitation within a $1^\circ \times 1^\circ$ gridbox binned by corrected ABI LWP and uncorrected ABI N_d . Mean precipitation rates are unconditional (i.e. include non-raining regions).

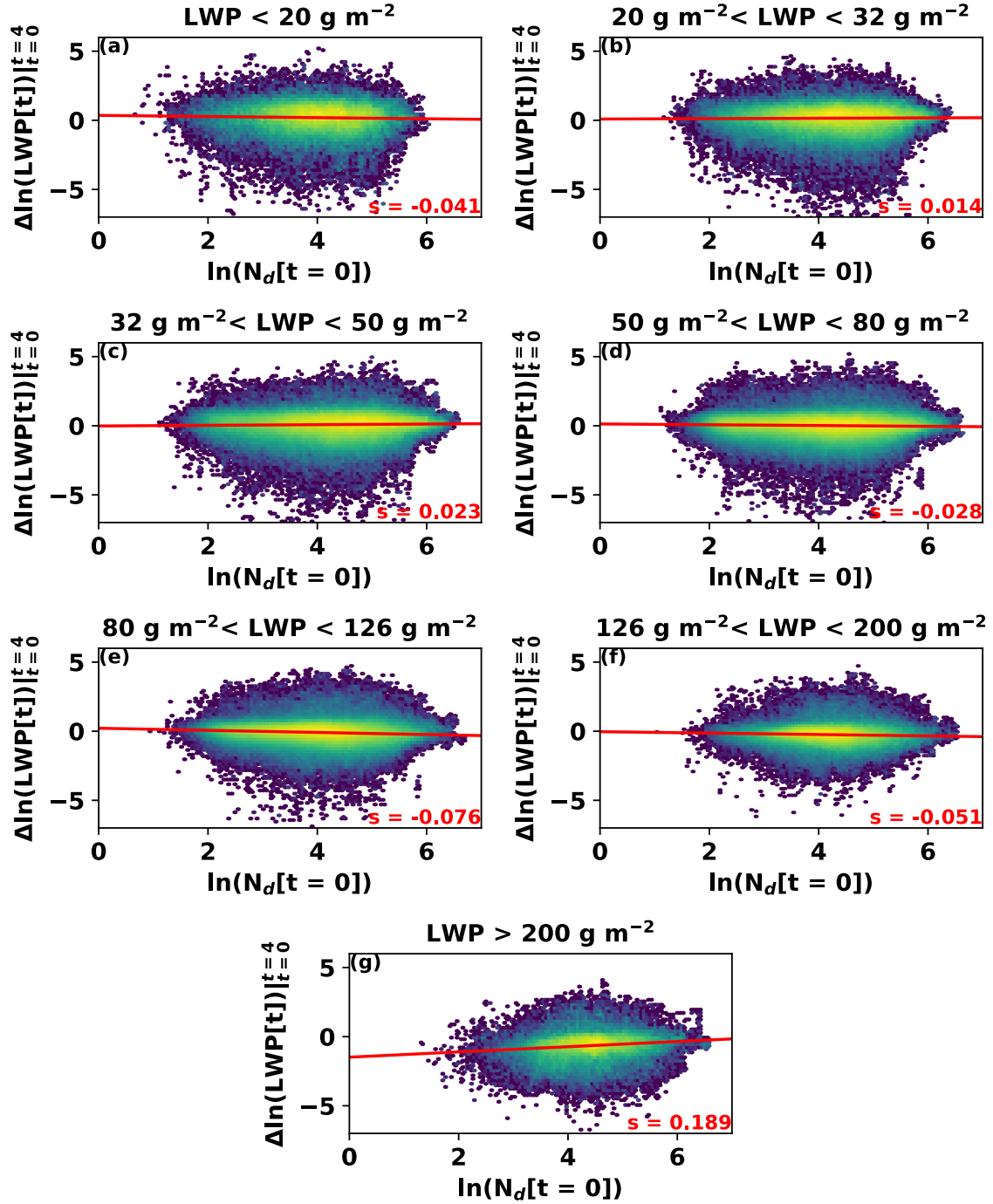


Figure S3: The difference between $\ln(\text{LWP}[\text{time} = 4 \text{ hrs}]) - \ln(\text{LWP}[\text{time} = 0 \text{ hrs}])$ for all trajectories conditioned by starting LWP are plotted against $\ln(N_d[\text{time} = 0 \text{ hrs}])$. s represents the slope of a fitted line which represents the λ we calculate and show at each time in Figure 1.

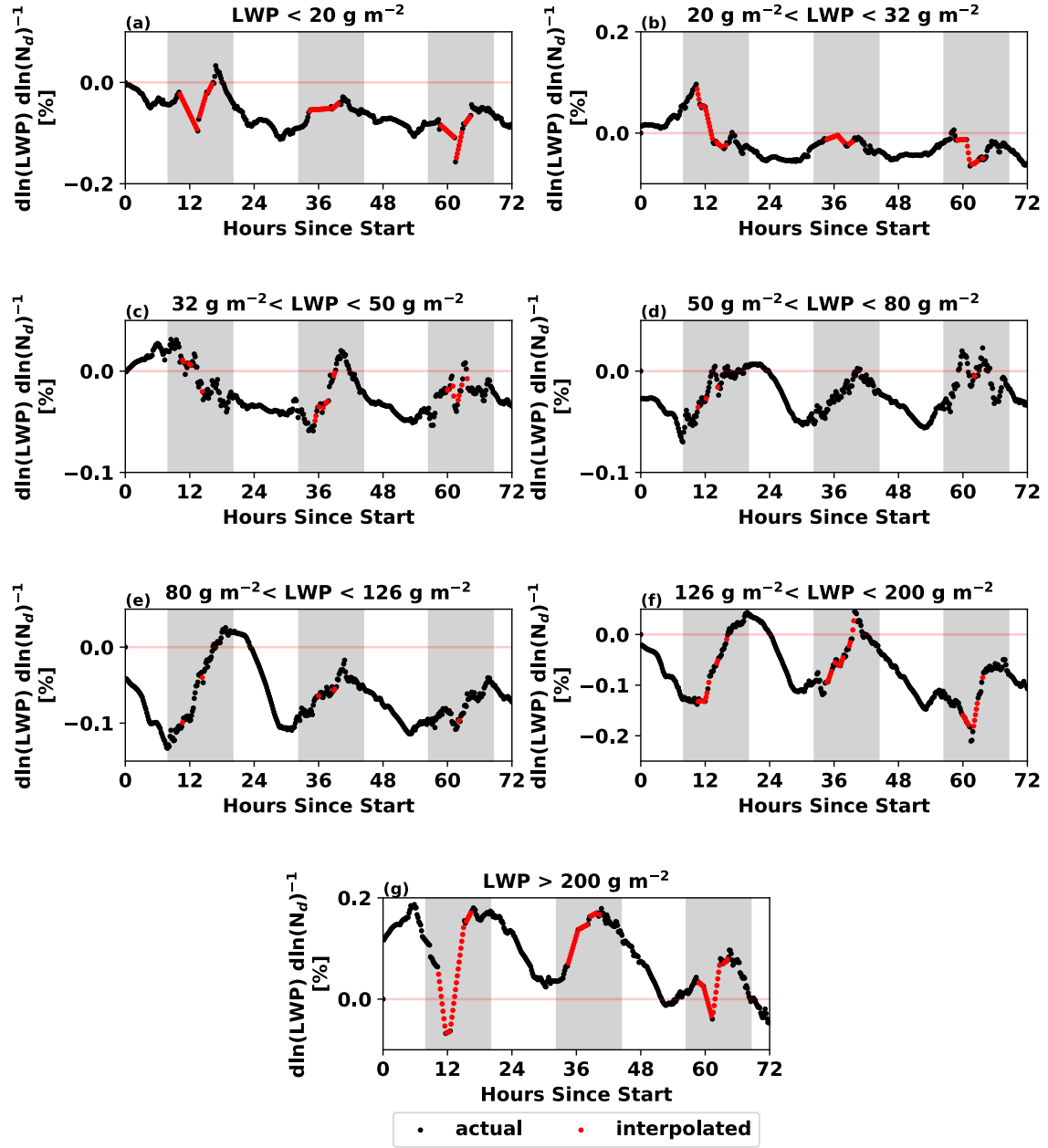


Figure S4: Each panel shows each individual curve in Figure 1, with the red points representing interpolated values. The white-filled regions represent day, and the grey-filled regions represent night.

Satellite	Orbit	Crossing Time (Local)	Duration
GMI	Non-Sun Synchronous	NA	2014-Prezent
AMSR-2	Sun Synchronous	13:33	2012-Present
SSMIS-F16	Sun Synchronous	16:27	2003-Present
SSMIS-F17	Sun Synchronous	18:35	2006-Present
SSMIS-F18	Sun Synchronous	16:30	2010-Present
WindSat	Sun Synchronous	18:10	2003-2020

Table S1. This table contains the six different microwave imagers used.

Table S2: *The λ values calculated in prior observational and LES studies shown in Figure 4. They are colored by if they represent non-precipitating (black), precipitating (red), or indiscriminate (blue) situations.*